COMPARATIVE EFFECTS BETWEEN NATURAL EXPOSURE AND ACCELERATED AGEING UNDER HYGROTHERMAL CONDITIONS AND UV RADIATION ON MODEL COMPOSITES MATRIX

T.H. NGUYEN[2], L. BELEC[1,*], J.F. CHAILAN[1], D.L. NGUYEN[2]

[1] *Laboratoire Matériaux Polymère Interface Environnement Marin (MAPIEM EA 4323), Université du Sud Toulon Var, ISITV BP56, 83162 La Valette du Var Cedex, France*
[2]*Danang University of Technology , Université de Danang, 54 Nguyen Luong Bang, Danang, Vietnam*
**belec@univ-tln.fr*

Keywords: natural ageing, accelerated ageing, force measurements

Abstract
A comparative study is performed on a simplified UD glass fibres composite exposed for several months in a natural environment on one hand, and to controlled hygrothermal and photo-degradation ageing tests in the laboratory on the other hand. Evidence of the hardener evaporation during curing is shown at sample surface in contact with air. The effects of different ageing conditions on this surface are characterized by analyzing successive layers (~ 20 µm) of resin by FTIR and DSC. Force measurements by Atomic Force Microscopy show an evolution of mechanical properties at composite surface function of ageing conditions.

1. Introduction

The validation of artificial ageing tests to reproduce and accelerate natural weathering conditions is necessary to study and predict the evolution of composite materials. The effects of UV radiation or hygrothermal stresses have often been considered separately but the combining effects, encountered in natural weathering conditions are not clear.
The photo-oxidation process of amine-epoxy resins has been widely described in the last decades [1][2][3][4][5]. It is generally admitted that the main photo-products for DGEBA-amine are carbonyls and amides, which may also be unstable under UV irradiation [3]. Photo-degradation propagation process mainly depends on amine concentration and nitrogen atom electron density [1]. The photo-oxidation processes of cured or uncured DGEBA are similar and lead to the formation phenyl formate end groups [4][5]. Moreover, photolysis of such systems results from the formation of a quinone methide structure. The photochemical removal of products during ageing has also been quantified using an ablation technique [2]. Competitive effects between chain scission and crosslinking processes under photo-oxidation were shown recently on phenoxy resins, thanks to nanoindentation and microhardness tests [6].
The effects of hygrothermal ageing on epoxy matrix are also well known in terms of water sorption, plasticizing effect, swelling phenomena, hydrolysis or formation of microcracks through absorption/desorption cycles [7][8][9][10]. The formation of physical crosslinks by water molecules is also reported [11]. It is well established that the most favourable hydrophilic site in epoxy–amine systems is the alcohol group of the hydroxypropylether sequences [12][13][14]. Perfectly crosslinked systems are generally resistant to hydrolysis but

when epoxyde groups are in excess and did not react with the amine of the hardener, they may react with water molecules to form diols which then form hydrogen bonds with other water molecules [13].
Artificial accelerated UV weathering may induce similar chemical changes in polymer matrix as those caused by natural exposure in sunny environments [15][16]. In these cases, photo-degradation is the main degradation process and is concentrated in the first tens micrometers. The main effect of precipitations on epoxy laminates is to leach out un-reacted constituents [17]. Cracks with low depth can be observed on the surface of the material after a few months of natural exposure in that case. A comparative study between natural exposure and artificial tests showed a saturation of the oxidizable groups by FTIR due to the loss of the oxidized products that were formed in the films [18].
The aim of the present study is to compare the effects of natural and artificial ageing conditions on a simplified epoxy-amine composite which surface shows incomplete curing. Classical physico-chemical characterization techniques are associated to force measurements by Atomic Force Microscopy to quantify and understand the surface effects of the different ageing conditions.

2. Materials and testing methods

2.1. Materials tested

The prepolymer is a diglycidyl ether of bisphenol A(DGEBA), n=0.13 and the hardener is a Diethylene Triamine (DETA). They were used in stoechiometric proportions.
The matrix is reinforced by E glass fibres reinforced by a simplified γ-APS sizing.
Unidirectional plates of 2 mm thickness with 20-25 % fibres were moulded with an optimized curing cycle to reach a maximum conversion rate (2 hrs at 60 °C followed by 2 hrs at 120 °C and 2 hrs at 140°C). The plates were exposed to UV radiation and natural ageing on the side in contact with air during the elaboration.
The material surface was scraped off progressively with a sharp blade on a precise surface to analyse it through its thickness. The collected chips were weighed to calculate the thickness of each removed layer.

2.2. Exposure environments

Specimens examined were exposed at Danang (16°10'N), Vietnam, for several months. The annual radiation was 6424 MJ/m^2 with a mean relative humidity (RH) of 82.3% (+/- 4 %). The mean maximum temperature was 29.8 °C (+/- 3.6 °C) with a mean minimum temperature value of 22.6 °C (+/- 2.3 °C). Samples were analyzed after 2, 4, 8, 12 and 19 months.
The accelerated weathering tests were performed on a QUV test chamber, using fluorescent lamps to provide a radiation spectrum centred in the ultraviolet A wavelengths (340 nm).The exposure temperature was 45 °C and the energy was fixed at 0.77 $W/m^2/nm$.
Samples were analysed after 3, 7, 15, 30 and 60 days exposure.
Hygrothermal ageing was performed at 70 °C, 85 % RH. The samples were analysed after 1, 2, 4 and 6 weeks.

2.3. Techniques

A differential scanning calorimeter (Q100) from TA Instrument was used to follow the glass transition temperatures evolutions. The powder from the different surface layers were analysed at 20 °C/min up to 200 °C. The glass transition was measured on the second cycle to eliminate relaxation effects.
FTIR spectra were collected using a Nexus FTIR spectrophotometer. All spectra were the coadditions of 64 scans taken at a resolution of 8 cm^{-1}.

AFM measurements were performed on a Nanoscope V controller equipped with a Multimode V Atomic Force Microscope, with a 8610 JVLR type scanner. Tapping mode cantilever probes (RTESP model from BRUKER) were used for the force measurements with a constant spring around 40 N/m. Each cantilever was systematically calibrated of a reference sample. The force curves were performed in tapping mode and the slope was calculated on the approach curves (between 0 and 50 nm of deflection) (Figure 1). The standard deviation is calculated on 10 measurements.
The samples are cut perpendicularly to fibre axis and polished up to 1µm with diamond grinding paste. Residues from polishing are eliminated by successive rinsing steps and compressed air drying.

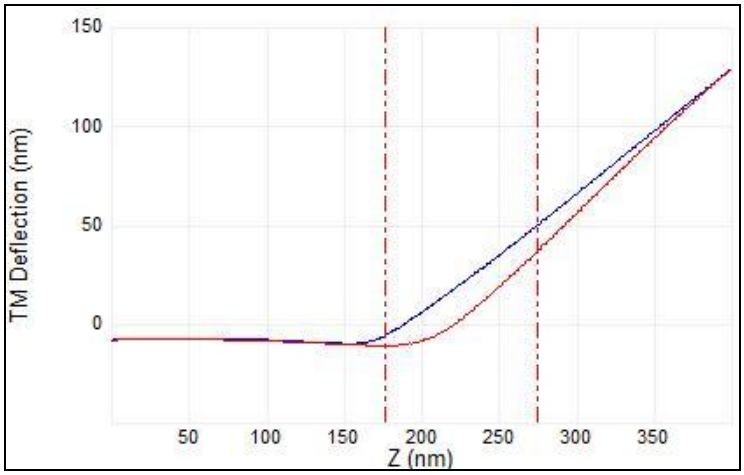

Figure 1. Determination of the slope on the approach force curve (AFM)

3 Results and discussion

3.1. Material at initial state

The composite at initial state shows a gradient in properties in the first 250 µm on the side which was in contact with air during curing (Figure 2). Indeed, the glass transition temperature increases from 90 °C in the first 20 µm thick layer up to 134°C at the centre and up to the opposite site of the plates (in contact with the mould). It must be noted that this area contains very few fibres.

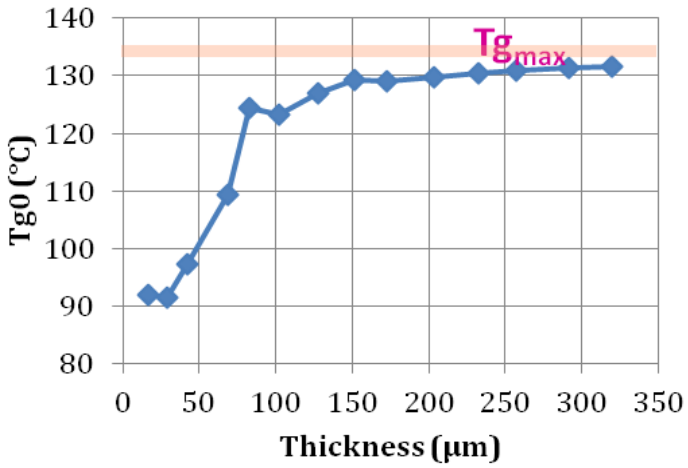

Figure 2. Evolution of the glass transition temperature from the surface at initial state (air side)

The evolution of Tg can be attributed to a gradient in crosslinks density, suggesting that the stoechiometric proportions were not respected near the surface during the plate curing.
FTIR analysis of the different layers, prepared in KBR pellets, show the presence of the unreacted oxirane band at 915 cm^{-1} which decreases progressively at increasing distance from the surface (Figure 3). This confirms that the conversion is partial and that amine is probably lacking near the surface. The evaporation of DETA around 105 °C was also showed by TGA measurements on the DGEBA/DETA mixture (not presented here).

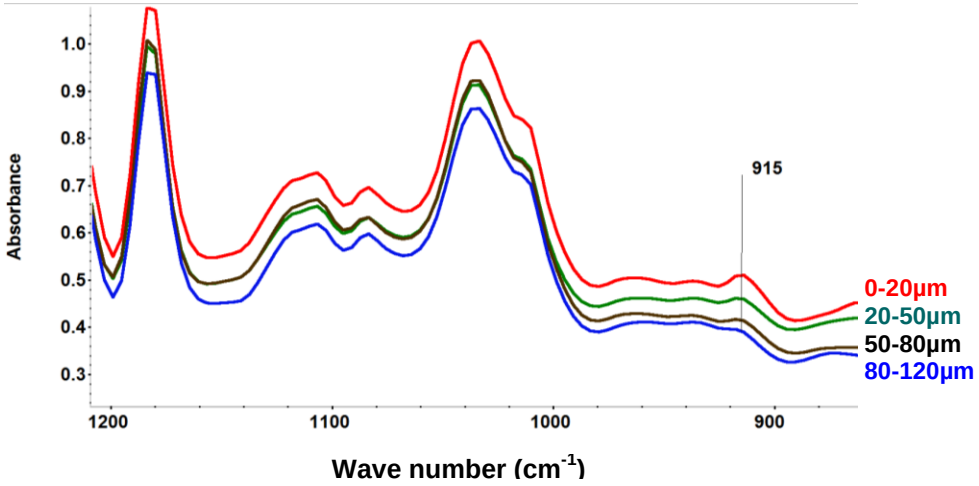

Figure 3 : FTIR analysis of matrix layers in KBR pellets. Evolution of oxirane band in the sample thickness for the initial composite plate (air side)

3.2.Comparison between the different ageing effects

FTIR analysis of the first 50 µm of the plates exposed to natural ageing during 4 months or to UV ageing during 60 days show similar evolutions in the carbonyle and amide regions. The trend is confirmed after 8 months of natural ageing. This is consistent with photo-oxidation of epoxy-amine systems described in literature [3][4] leading to ketone and formate around 1730-1740 cm^{-1} [5] and to amide or quinone methide groups around 1650-1660 cm^{-1}. Moreover, a decrease of oxirane band is observed in both cases, suggesting an epoxide oxidative ring-opening by UV radiation. The surface erosion limited to a few micrometers [2] is neglected in this analysis.

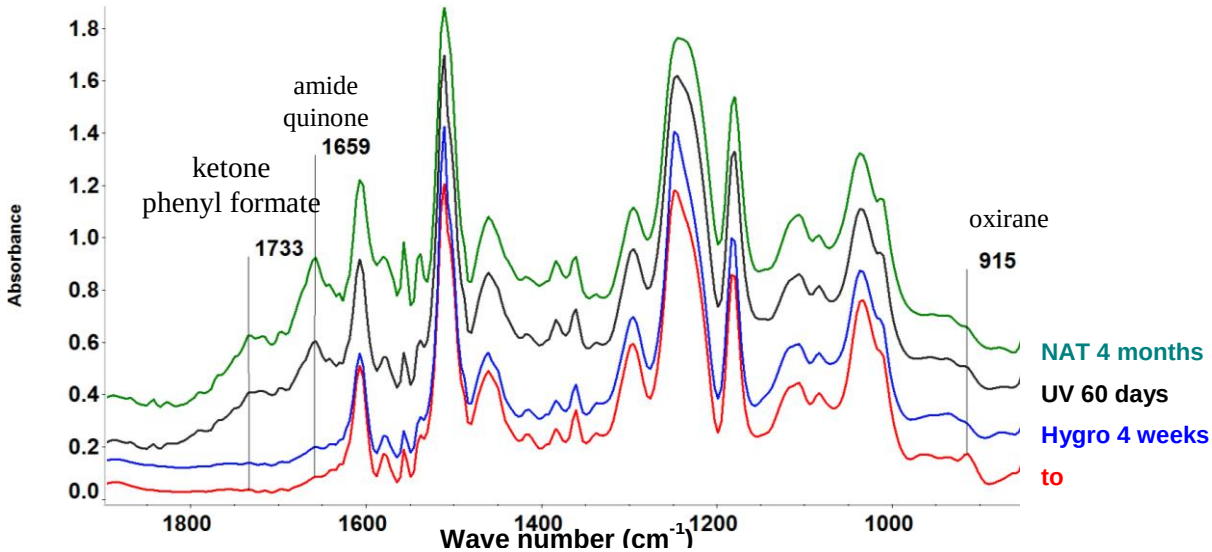

Figure 4 . Comparison between ageing in natural conditions, hygrothermal and UV ageing on 0-10 µm surface layer

The effect of hygrothermal ageing on FTIR spectra in the first layer mainly concerns the oxirane band which also decreases after 28 days. This can be attributed to the epoxy ring hydrolysis.

Figure 5 shows the different ageing effects on the resin mobility at increasing distance from the surface (initially in contact with air). All ageing conditions imply an increase of Tg in the first 20 µm, especially after hygrothermal ageing (over 200 µm). It must be noted that the Tg is measured on the 2nd cycle and that reversible water plasticizing effects are partially eliminated. The huge increase during hygrothermal ageing can be attributed to crosslinking effects following the epoxy-ring opening as observed on FTIR spectra. Epoxyde groups in excess may indeed react with water molecules and form hydrogen bonds leading to physical crosslinking processes [11][13]. These bonded water molecules may not be desorbed during the 1rst cycle.

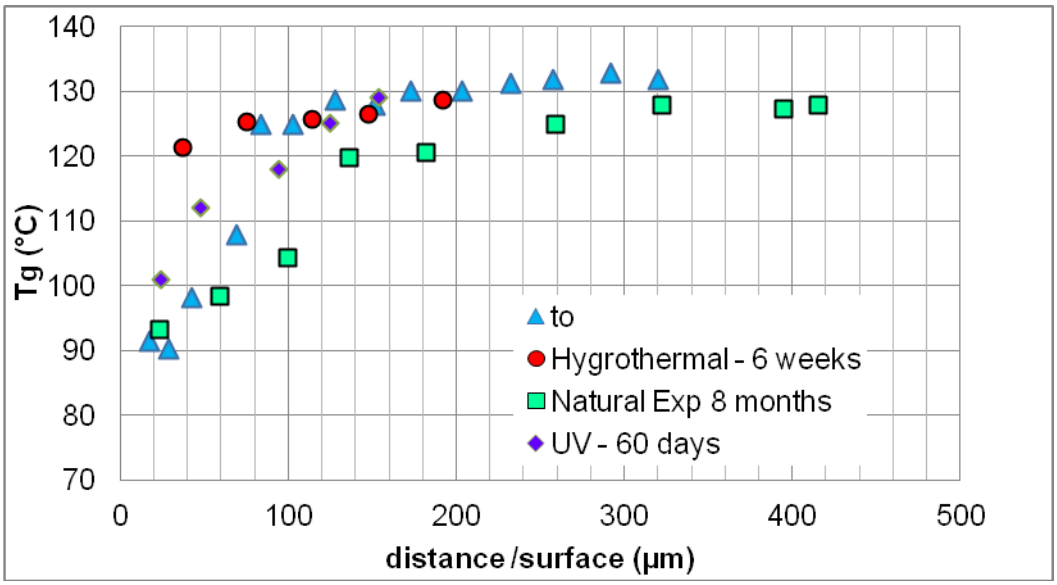

Figure 5. Influence of different ageing conditions on Tg, measured by DSC at 20 °C/min at increasing distance from the surface.

UV ageing also increases the Tg compared to initial state in the first 70 µm which is not consistent with a single chain scission photo-oxidative process. Crosslinking reactions may take place as observed in other systems [6] and as suggested by the decrease of the epoxy rings.
Nevertheless, the effects of natural ageing and UV ageing are quite different in terms of molecular mobility. If photoproducts are similar in the first layers, as observed on FTIR spectra, the network is softened over 300 µm after 8 months of natural ageing (Tg lower than the initial Tg between 60 and 300 µm). This evolution, completely at the opposite of UV or hygrothermal effects, suggests combined degradation processes. During natural ageing, UV radiation probably increases the epoxy network hydrolysis.

To get further information on these surface effects, force measurements are then performed in the same area, but with a higher resolution. Successive areas of 20x20 µm^2 are scanned in tapping mode and force measurements are performed with steps of 1 µm from the surface.
The reported results correspond to the slope calculated in the linear range (0-50 nm), on deflection versus sample vertical displacement approach curve.

The results show an important evolution during ageing conditions in the first 20 µm, especially considering UV ageing after 60 days (Figure 6). An increase of the stiffness is even observed in the first 10 µm. This result seems to confirm the hypothesis of competitive effects between chain scission photo-oxidative process, deduced from FTIR analysis, and crosslinking reactions as suggested by the increase in Tg and the decrease in oxirane ring. Further analysis is required to precise these mechanisms.
The effects of hygrothermal ageing on surface apparent stiffness are less important than the effects on Tg. It probably results from the plasticizing effects of water which are detectable during the force measurement test since no water desorption occurs. These plasticizing effects may be in competition with the physical crosslinking processes suggested by DSC measurements.
The surface stiffening is limited in the case of natural ageing compared to UV or hygrothermal ageing. This result confirms possible synergy effects during natural ageing, with the hydrolysis of epoxy-amine network under natural UV radiation.

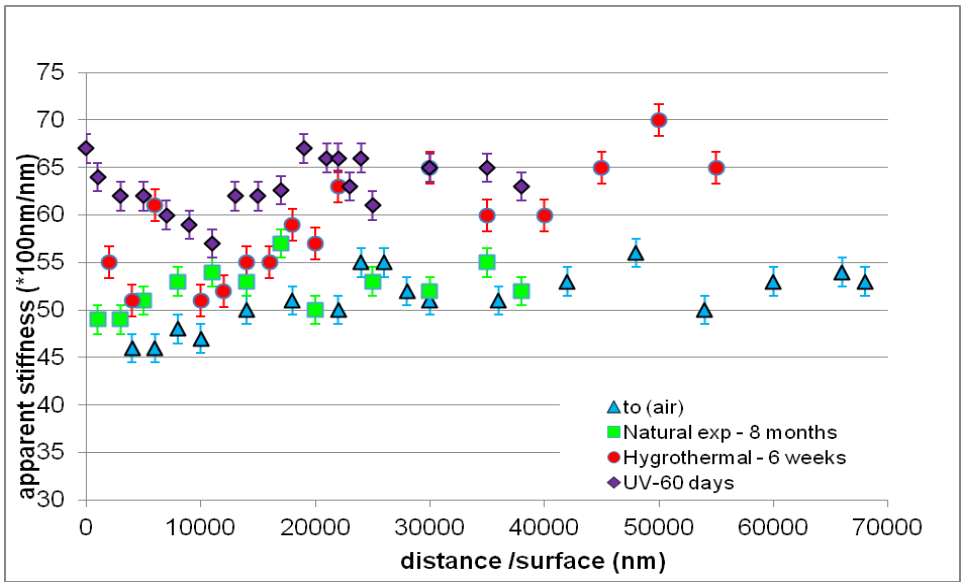

Figure 6. Evolution of composite apparent stiffness measured by AFM local force measurements at increasing distance from the surface (nm) after different ageing tests

4 Conclusion

The present study shows up the effects of incomplete curing of epoxy-amine networks on different ageing processes. The excess of unreacted polyepoxyde in the first 250µm leads to competitive effects between chain scission photo-oxidative process and crosslinking reactions during artificial UV ageing. In the case of hygrothermal ageing, plasticizing effects may be in competition with physical crosslinking processes. The different methods show synergy effects during natural ageing conditions leading to a probable hydrolysis of the epoxy-amine network at the surface due to the combination of hygrothermal conditions and UV radiation.
Force measurements method gives accurate evolutions in the first 10 µm, which were impossible to obtain by the ablation technique. Moreover, contrarily to DSC analysis, desorption of water molecules is very limited during the test, which makes the method interesting to characterize ageing effects.
The force measurement method is now applied to the characterization of interphases of the UD composite and to follow their evolution during ageing.

References

[1] Bellenger V., Verdu J., *Journal of Applied Polymer Science*, **28**, pp. 2677-2688 (1983)
[2] Guillot L., Monney L., Dubois C., Chambaudet A., *Polymer Degradation and Stability*, **72**, pp. 209-215 (2001)
[3] Delor-Jestin F., Drouin D., Cheval P.-Y., Lacoste J., *Polymer Degradation and Stability* **91**, pp. 1247-1255 (2006)
[4] Rivaton A, Moreau L, Gardette J-L. *Polymer Degradation and Stability*, **58**, pp.333-339 (1997)
[5] Mailhot B., Morlat-Therias S., Ouahioune M., Gardette J.L., *Macromolecular Chemistry and Physics*, **206**, pp. 575-584 (2005)
[6] Larché J.-F., Bussière P.-O., Thérias S., Gardette J.-L., *Polymer Degradation and Stability*, **97**, pp. 25-34 (2012)
[7] Adamson MJJ. *Journal of Materials Science*, **15**, pp.1736-1745. (1980)
[8] Xiao G.Z., Shanahan M.E.R., *Journal of polymer Science Part B*, **35**, pp. 2659-2670 (1997)
[9] Perrin F.X., Nguyen M.H., Vernet J.L., *European Polymer Journal*, **45**, pp.1524-1534 (2009)
[10] Browning C.E., *Polymer Engineering and Science*, **18**, pp.16-24 (1978)
[11] Zhou J., Lucas J.P., *Polymer*, **40**, pp.5513-5522 (1999)
[12] Mijovic J., Zhang H., *The Journal of Physical Chemistry B* ,**108**, pp.2557-2563, (2004)
[13] Popineau S., Rondeau-Mouro C., Sulpice-Gaillet C., Shanahan M.E.R., *Polymer*, **46**, pp. 10733-10740 (2005)
[14] Musto P., Ragosta G., Mascia L., *Chemistry of Materials*,**12**, pp.1331-1341 (2000)
[15] Bauer D.R., Mielewski D.F., Gerlock J.L., *Polymer Degradation and Stability*, **38**, pp. 57-65 (1992)
[16] Merlatti C., Perrin F.X., Aragon E., Margaillan A., *Polymer Degradation and Stability* , **93**, pp. 896-903 (2008)
[17] Sookay N.K., Von Klemperer C.J., Verijenko V.E., *Composite Structures*, **62**, pp. 429-433 (2003)
[18] Rezig A., Nguyen T., Martin D., Sung L., Gu X, Jasmin J., *JCT Research*, **3**, pp. 173-184 (2006)